

**DEVELOPMENT OF A FDTD SIMULATION OF
IONOSPHERE PROPAGATION FOR
EARTHQUAKE PRECURSOR OVER THE
SUMATERA-MALAYSIA REGION**

by

SITI HARWANI MD YUSOFF

**Thesis submitted in fulfilment of the requirements
for the degree of
Doctor of Philosophy**

September 2018

ACKNOWLEDGEMENT

First and foremost, praises and thanks to the God, the Almighty, for His showers of blessings throughout my research work to complete the research successfully.

I would like to express my deep and sincere gratitude to my research supervisor, Assoc. Prof. Dr. Yoon Tiem Leong, for giving me the opportunity to do research and providing invaluable guidance throughout this research. His dynamism, vision, sincerity, and motivation have deeply inspired me. It was a great privilege and honour to work and study under his guidance. I would like to say thank you for my co-supervisor, Assoc. Prof Dr. Lim Hwee San for his advice and support throughout this research work.

I am extremely grateful to my husband, Mohd Ikhwan, who has helped to ease some of the burdens and pressures of the Ph.D. Without his love and continuing support, I would not able to complete my Ph.D. journey. He has always been there to offer reassurance during the difficult times and to celebrate my successes. I appreciate the sacrifices he has made so I could attain this degree. Also, I express my thanks to my 3 adorable children, the reason why I am not giving up in the middle of the journey. I would like to thank my parent, mother-in-law, and my siblings for their prayers and borderless love.

I am extending my acknowledgment to my colleagues and staff in School of Aerospace Engineering, Universiti Sains Malaysia for all the support. Special thanks to Dr. Norilmi Amilia and Dr. Aslina, for their support and valuable advices during

my ups and downs, my Dean, Prof Ir. Dr. Mohd Zulkifly Abdullah, and my Program Chairman, Ir. Dr. Nurulasikin for their understanding.

Finally, my thanks go to all the people who have supported me to complete the research work directly or indirectly. For those who answer the call for help in the middle of the day and night, near and from far, with no expectation of personal gain. This thesis would not have been possible without them.

I would like to acknowledge the Ministry of Higher Education (MOHE) and Universiti Sains Malaysia for granted scholarship under the Academic Staff Higher Education Scheme (ASHES).

TABLE OF CONTENTS

Acknowledgement	ii
Table of Contents	iv
List of Tables	viii
List of Figures	ix
List of Symbols	xiv
List of Abbreviations	xvi
Abstrak	xviii
Abstract	xx
CHAPTER 1 INTRODUCTION	1
1.1 Overview	1
1.2 Ionospheric Physics	3
1.3 The electromagnetic signal	4
1.4 FDTD Modelling	5
1.5 Research questions	7
1.6 Problem Statements	8
1.7 Research Objectives	9
1.8 Scope of Study	10
1.9 Significance of the Study	11
1.10 Originality Contribution	13

1.11	Organization of Chapter	13
CHAPTER 2 LITERATURE REVIEW		15
2.1	Ionosphere and Ionospheric Disturbance	15
2.2	The Ionospheric Parameter	17
2.3	Seismo-ionospheric Coupling	20
2.4	The E-layer of Ionosphere	23
2.5	The CHAMP Satellite	24
	2.5.1 The CHAMP Radio Occultation Technique	25
2.6	The IRI Model	26
2.7	FDTD Modelling of Earth-Ionosphere	26
2.8	Absorbing Boundary Condition	30
2.9	Summary on Literature Review	30
CHAPTER 3 METHODOLOGY		32
3.1	The Data Collection	32
3.2	The FDTD Formulation	33
3.3	Implementation Of Absorbing Boundary Condition	41
3.4	Codes Verification	49
3.5	Summary	52
CHAPTER 4 ELECTRON DENSITY PROFILE IDENTIFICATION NEAR THE EARTHQUAKE ACTIVE REGION IN SOUTHEAST ASIA		53

4.1	Introduction	53
4.2	Space Weather Condition on December 2004	53
4.3	Observation on Electron Density Profile before the Sumatera-Aceh 2004 Earthquake	56
4.4	The Electron Density Profile from Satellite Source and the IRI Empirical Model	60
4.5	Summary	62
CHAPTER 5 FDTD ABSORBING BOUNDARY CONDITION IN IONOSPHERIC MEDIUM		64
5.1	Introduction	64
5.2	Numerical Experiment with ABC	64
5.3	Numerical Experiment with Perfectly Matched Layer (PML)	73
5.4	Performance of PML with Varying Thickness	79
5.5	2D FDTD Code Verification	84
5.6	Summary	87
CHAPTER 6 ELECTROMAGNETIC WAVE PROPAGATION IN LOCAL IONOSPHERE		89
6.1	Introduction	89
6.2	Analysis of the Transient E_z Component in the Presence of N_e based on Satellite Data	91
6.3	Quantifying the Amplitude Difference in the Transient Electric Field, E_z	98
6.4	ΔQ_s as an Earthquake Precursor	106
6.5	Summary	111

CHAPTER 7 CONCLUSIONS AND FUTURE WORKS	113
7.1 Conclusions and Findings	113
7.2 Future Works	115
REFERENCES	118
APPENDIX	
LIST OF PUBLICATIONS	

LIST OF TABLES

		Page
Table 3.1	The days and time when the satellite data were collected	32
Table 3.2	Information of the Sumatera-Andaman Island earthquake	33
Table 3.3	PML absorber parameters and the range	45
Table 3.4	Main parameters of the FDTD and PML parameters	47

LIST OF FIGURES

		Page
Figure 1.1	The earthquake with magnitude 6 and more occurred in South East Asia within 1997 until 2017.	2
Figure 1.2	The location of earthquake epicentre in Sumatra region.	3
Figure 1.3	The electromagnetic wave propagation from a ground source through the atmosphere up to a height of 120 km where the ionosphere resides.	7
Figure 2.1	Physical mechanism of seismo-ionospheric coupling.	21
Figure 3.1	The electric field, E_z , current density, J_z and magnetic field, H_x and H_y in interface of the fields	38
Figure 3.2	Two-dimensional computational grids for wave propagation. The shaded stripes along the edges are grid layers where ABC is to be implemented.	43
Figure 3.3	The location of the sites in which the relative error of the electric field is accessed.	48
Figure 3.4	Flow-chart of the FDTD algorithm.	51
Figure 4.1	Solar flux F10.7 on December 2004	55
Figure 4.2	Kp index for December 2004	55
Figure 4.3	Dst index for middle of December 2004	56
Figure 4.4	Variations of the electron density a few days before the earthquake. (a) 21 st December, 2004 at 13:03 LTC at label 1 and 22 nd December, 2004 at 00:35 LTC at label 2, (b) 23 rd	57

	December, 2004 at 11:00 LTC at label 1, 24 th December, 2004 at 00:01 LTC at label 2 and 24 th December, 2004 at 23:03 LTC at label 3.	
Figure 4.5	Variation in the electron density profile on (a) 25 th December 2004 at 10:31 LTC on label 1, at 23:29 LTC on label 2 and 26 th December 2004 at 12:33 LTC on label 3.	59
Figure 4.6	Comparison of the electron density profile by CHAMP satellite and IRI 2012 model.	62
Figure 5.1	E_z field components for ABC after 2000 steps	65
Figure 5.2(a)	Relative errors at site A within 2000 time-steps using ABC	69
Figure 5.2(b)	Relative errors at site B within 2000 time-steps using ABC	69
Figure 5.2(c)	Relative errors at site C within 2000 time-steps using ABC	70
Figure 5.2(d)	Relative errors at site D within 2000 time-steps using ABC	70
Figure 5.2(e)	Relative errors at site E within 2000 time-steps using ABC	71
Figure 5.2(f)	Relative errors at site F within 2000 time-steps using ABC	71
Figure 5.2(g)	The grouping of all sites	72
Figure 5.3	E_z field component for 25 cells of PML after $n = 2000$ steps.	73
Figure 5.4(a)	Relative error at site A within 2000 time-steps using Perfectly Matched Layer.	75
Figure 5.4(b)	Relative error at site B within 2000 time-steps using Perfectly Matched Layer.	75
Figure 5.4(c)	Relative error at site C within 2000 time-steps using Perfectly Matched Layer.	76

Figure 5.4(d)	Relative error at site D within 2000 time-steps using Perfectly Matched Layer.	76
Figure 5.4(e)	Relative error at site E within 2000 time-steps using Perfectly Matched Layer.	77
Figure 5.4(f)	Relative error at site F within 2000 time-steps using Perfectly Matched Layer.	77
Figure 5.4(g)	The grouping of all sites.	78
Figure 5.5(a)	Relative errors at site F for 5 PML cells at 2000 time steps.	80
Figure 5.5(b)	Relative errors at site F for 10 PML cells at 2000 time steps.	80
Figure 5.5(c)	Relative errors at site F for 15 PML cells at 2000 time steps.	81
Figure 5.5(d)	Relative errors at site F for 20 PML cells at 2000 time steps.	81
Figure 5.5(e)	Relative errors at site F for 25 PML cells at 2000 time steps.	82
Figure 5.5(f)	Grouping of all relative errors.	82
Figure 5.6	The values of relative error amplitude at thickness $N_{\text{PML}} = 5, 10, 15, 20, 25$ in the PML implemented in the anisotropic ionospheric medium at site F.	84
Figure 5.7	Vertical Electric field for free space and anisotropic condition probe at site 2 ($i = 500, j = 4$).	86
Figure 6.1	The location of sites 1,2 and 3 in computational grid.	90
Figure 6.2	The transient E_z field component in free space condition at measured in sites 1, 2 and 3.	93

Figure 6.3(a)	The transient E_z field component collected on 21 st Dec 2004, 13:03 LTC	94
Figure 6.3(b)	The transient E_z field component collected on 21 st Dec 2004, 00:35 LTC	94
Figure 6.3(c)	The transient E_z field component collected on 23 rd Dec 2004, 11:00 LTC	95
Figure 6.3(d)	The transient E_z field component collected on 23 rd Dec 2004, 00:01 UTC	95
Figure 6.3(e)	The transient E_z field component collected on 24 th Dec 2004, 23:03 LTC	96
Figure 6.3(f)	The transient E_z field component collected on 25 th Dec 2004, 10:31 LTC	96
Figure 6.3(g)	The transient E_z field component collected on 25 th Dec 2004, 23:29 LTC	97
Figure 6.3(h)	The transient E_z field component collected on 26 th Dec 2004, 12:33 LTC	97
Figure 6.4(a)	Time domain in which the difference in the amplitudes of transient electric field in free space (1) and anisotropic, dispersive medium (2) at site 1 is enumerated.	99
Figure 6.4(b)	Time domain in which the difference in the amplitudes of transient electric field in free space (1) and anisotropic, dispersive medium (2) at site 2 is enumerated.	99
Figure 6.4(c)	Time domain in which the difference in the amplitudes of transient electric field in free space (1) and anisotropic, dispersive medium (2) at site 3 is enumerated.	100

Figure 6.5(a)	(1) The electron density profile on 21 st Dec 2004, 13:03 LTC (2) The amplitude difference at sites 1, 2 and 3.	102
Figure 6.5(b)	(1) The electron density profile on 22 nd Dec 2004, 00:35 LTC (2) The amplitude difference at sites 1, 2 and 3.	102
Figure 6.5(c)	The electron density profile on 23 rd Dec 2004, 11:00 LTC (2) The amplitude difference at sites 1, 2 and 3.	103
Figure 6.5(d)	(1) The electron density profile on 24 th Dec 2004, 00:01 LTC (2) The amplitude difference at sites 1, 2 and 3.	103
Figure 6.5(e)	(1) The electron density profile on 24 th Dec 2004, 23:03 LTC (2) The amplitude difference at sites 1, 2 and 3.	104
Figure 6.5(f)	(1) The electron density profile on 25 th Dec 2004, 10:31 LTC (2) The amplitude difference at sites 1, 2 and 3.	104
Figure 6.5(g)	(1) The electron density profile on 25 th Dec 2004, 23:29 LTC (2) The amplitude difference at sites 1, 2 and 3.	105
Figure 6.5(h)	(1) The electron density profile on 26 th Dec 2004, 12:33 LTC (2) The amplitude difference at sites 1, 2 and 3.	105
Figure 6.6(a)	$\Delta Q_{s=2}$ as a function of the date when electron density data were taken.	109
Figure 6.6(b)	$\Delta Q_{s=3}$ as a function of the date when electron density data were taken.	109
Figure 7.1	The FDTD development and future tasks.	116

LIST OF SYMBOLS

Ap index	Planetary A-index
B	Magnetic Flux Density
B_0	Earth's natural magnetic field
c_0	Speed of light
C_{ax}, C_{bx}	Coefficients for electric field
D_{ax}, D_{bx}	Coefficients for magnetic field in x-direction
D_{ay}, D_{by}	Coefficients for magnetic field in y-direction
Dst index	Disturbance Storm Time index
E	Electric Field
E_0	E_z component at source
E_{ref}	Values of E_z measured in the reference domain
$E_{ref,max}$	Maximum values of E_z measured in the reference domain
E_z	Electric Field in z-direction
f_0	Frequency
foF2	Critical frequency of the F2 layer of the ionosphere
h	Height
H	Magnetic Field
H_x	Magnetic Field in x-direction
H_y	Magnetic Field in y-direction
h	User-defined rate of growth
i,j	Temporal and spatial discretization
J	Electric Current Density
J_z	Electric Current Density in z-direction
k	Spatial index
Kp index	Planetary K-index

m	Particle Mass
m_e	Electron mass
n	time step
N	Positive real or positive integer of n
N_e	Electron Density
N_{PML}	PML thickness
q	Particle Charge
R_0	Reflection coefficient
t	Temporal Variable
ϑ	Velocity
β	User-defined difference in the exponent rates
Δ	Spatial width
δk	Thickness of the PML in the grid index by
ΔQ	Root Mean Square of E_z
Δx	Spatial width in x-direction
Δy	Spatial width in y-direction
ε_0	Permittivity of free space
ε_{max}	User-defined parameter to control the rate of evanescent mode attenuation
μ_0	Permeability of free space
ν	Electron Collision Frequency
ρ_k	Depth in PML
σ, σ^*	Conductivity
ω_b	Gyro Frequency or Cyclotron Frequency
ω_p	Plasma Frequency
ω_r	Angular Conductivity

LIST OF ABBREVIATIONS

2D	2-Dimensional
ABC	Absorbing Boundary Condition
ADE	Auxiliary Differential Equation
AGW	Acoustic Gravity Wave
CHAMP	Challenging Minisatellite Payload
CFL	Courant-Friedrich-Lewis
COSPAR	Committee of Space Research
EEJ	Equatorial Electrojet
EIA	Equatorial Ionization Anomaly
ELF	Extreme Low Frequency
EM	Electromagnetic
FDTD	Finite Difference Time Domain
GPS	Global Positioning System
GPS-MET	Global Positioning System/Meteorology
GPS-TEC	Global Positioning System - Total Electron Content
GRACE	Gravity Recovery and Climate Experiment
HF	High Frequency
IAGA	International Association of Geomagnetism and Aeronomy
IGRF	International Geomagnetic Reference Field
IRI	International Reference Ionosphere
ISDC	Information System and Data Centre
LEO	Low Earth Orbit

PLCDRC	Piecewise Linear Current Density Recursive Convolution
PML	Perfectly Matched Layer
RAM	Random Access Memory
RC	Recursive Convolution
RO	Radio Occultation
SAC-C	Satellite de Aplicaciones Cientificas-C
S-FDTD	Stochastic Finite Difference Time Domain
TEC	Total Electron Content
TM	Transverse Magnetic
ULF	Ultra Low Frequency
URSI	International Union of Radio Science
UTC	Coordinated Universal Time
VLF	Very Low Frequency
VLF-LF	Very Low Frequency-Low Frequency

PEMBANGUNAN SIMULASI FDTD BAGI PERAMBATAN IONOSFERA UNTUK PREKUSOR GEMPA BUMI DI RANTAU SUMATERA-MALAYSIA

ABSTRAK

Gangguan di dalam medan elektrik menegak di ionosfera sebelum berlakunya gempa bumi yang besar sangat kurang dikaji. Maklumat medan elektrik menegak yang diperolehi daripada gelombang eletromagnetik (EM) yang merambat melalui ionosfera boleh diaplikasikan untuk membina prekursor gempa bumi. Kajian ini dijalankan melalui pembangunan kod 2D Perbezaan Terhad Domain Masa (FDTD) untuk simulasikan perambatan EM di dalam ionosfera yang anisotropic. Untuk meniru keadaan ionosfera yang anisotropik dan menyebar, profil ketumpatan elektron (N_e) yang dikutip daripada satelit CHAMP digunakan di dalam kod sebagai parameter untuk medium. Data yang digunakan di dalam kod ini adalah 5 hari sebelum berlakunya gempa bumi Lautan Andaman di Aceh pada 26 Disember 2004. Lapisan Padan Sempurna (PML) sebagai sempadan penyerapan digunakan di dalam kod ini untuk memastikan gelombang yang memantul daripada sempadan adalah minimum. Berdasarkan data yang dihasilkan daripada simulasi FDTD ini, satu protocol untuk prekursor gempabumi, dikenali sebagai ΔQ dibina. Keputusannya, gangguan di dalam profil ketumpatan electron dikesan 3 hari sebelum berlakunya gempa bumi besar, ditunjukkan melalui nilai N_e yang tinggi di dalam profil. Sebagai tambahan, ada 1 hari sebelum kejadian gempa bumi menunjukkan profil yang terganggu. Medan elektrik menegak daripada perambatan electromagnet menggunakan kaedah FDTD dibangunkan dan menunjukkan tahap kepekaan yang tinggi terhadap perubahan medium di ionosfera. Kejituan PML juga diukur melalui

pengiraan ralat relative. Keputusan menunjukkan 25 sel untuk PML boleh menahan pantulan gelombang 48% lebih baik dari 5 sel untuk PML. Kemudian, kerana kekurangan data N_e , tiada kesimpulan ramalan yang boleh dilakarkan daripada pengiraan ΔQ . Walaubagaimanapun, ciri-ciri daripada plot ΔQ memberi petanda satu puncak ditunjukkan sebelum berlakunya gempa bumi. Kesimpulannya, secara teknikalnya kita berupaya untuk mengunakan parameter ionosfera ke dalam komputasi electromagnet sebagai cubaan untuk menghasilkan prekursor gempa bumi.

**DEVELOPMENT OF A FDTD SIMULATION OF IONOSPHERE
PROPAGATION FOR EARTHQUAKE PRECURSOR OVER THE
SUMATERA-MALAYSIA REGION**

ABSTRACT

The perturbation on the vertical electric field in the ionosphere before large the large earthquake is a poorly investigated problem. The information obtaining from the electromagnetic (EM) wave propagated through the ionosphere can be applied to construct an earthquake precursor. This study conducted through the development of a home-grown 2D Finite Difference Time Domain (FDTD) code to simulate the EM propagation in the anisotropic ionosphere. To imitate the anisotropic and dispersive condition of the ionosphere, the electron density (N_e) profile collected from the CHAMP satellite is applied in the code as the medium parameter. The data used in this code is from 5 days before Aceh 2004 Andaman Sea earthquake, occurred on 26th December 2004. Perfectly Matched Layer (PML) as an absorbing boundary condition is implemented in the code to ensure minimum wave reflected from the boundary of the computational grid. Based on data generated from the FDTD simulation, a protocol for an earthquake precursor, known as ΔQ is constructed. As results, some perturbations in electron density profile are observed 3 days before the large earthquake occurred, shown in the high value of N_e in the profile. In addition, a day shows a distorted profile. The vertical electric field from EM propagation using FDTD simulation is developed and shows good sensitiveness to the change of the medium in the ionosphere. The PML efficiency is measured through the relative error calculation. The results show 25 cells of PML can suppress

the reflective wave 48% better than 5 cells of PML. Due to the lack of data on N_e , no conclusive prediction can be drawn from the measurement of ΔQ . However, the feature of ΔQ plot alone hinted a peak before at the occurrence of the earthquake. As a conclusion, it is technically viable to couple ionospheric parameter into the computational electromagnetic simulation as an attempt to develop an earthquake precursor.

CHAPTER 1

INTRODUCTION

1.1 Overview

Earthquake is a phenomenon where the tectonic plate of Earth moves either horizontally or vertically due to the activity of Earth's crust or volcanic activity and release sudden energy known as seismic waves. This incident called seismic event, and when the tectonic plates move, the Earth's surface is shaking and cause ground displacement. The earthquake magnitude can be measured using a seismometer, and the unit is on the Richter scale. Large earthquakes with more than 7 Richter magnitude scale potentially cause damages of buildings, injury or loss of life, landslides, fires and some studies show earthquake with 7 and more magnitude that occurred on the seabed, the movement of the seabed can produce sudden movement of large volumes of water called the tsunami.

In past 20 years, the earthquake event with magnitude 6 and more occurred in average 30 events per year as shown in Figure 1.1, prompting good motivation to conduct a research on modelling earthquake precursors. One of the approaches is via computational modelling of electromagnetic wave signal propagating in the ionosphere.

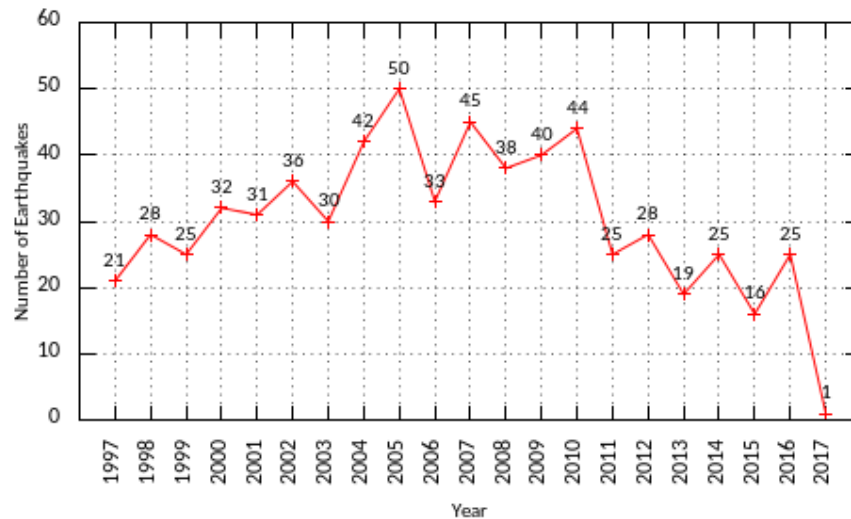


Figure 1.1 The earthquake with magnitude 6 and more occurred in South East Asia from 1997 until 2017

(Page URL: <https://earthquake.usgs.gov/earthquakes/search/> , downloaded on 31st Jan 2018)

The idea of seismo-ionospheric coupling is to study the connection between ionospheric perturbation and seismic activity during earthquake preparation process. This study is multidisciplinary and needs a wide range of knowledge in very specific disciplines, covering areas ranging from Earth plate tectonics deep down to Earth’s magnetosphere high up.

Referring to Figure 1.2, the epicentre areas in the Andaman Sea focuses on the northern region of Sumatra. It demonstrates how easily this plate can be ruptured. Before 2004, the seismologist community did not positively anticipate the region to be hit by a massive earthquake of such a scale. This event is chosen as our case study since it left major impacts on the socio-economy of Malaysia.

Seismicity of the Northeast Indian Ocean 1900 - 2004

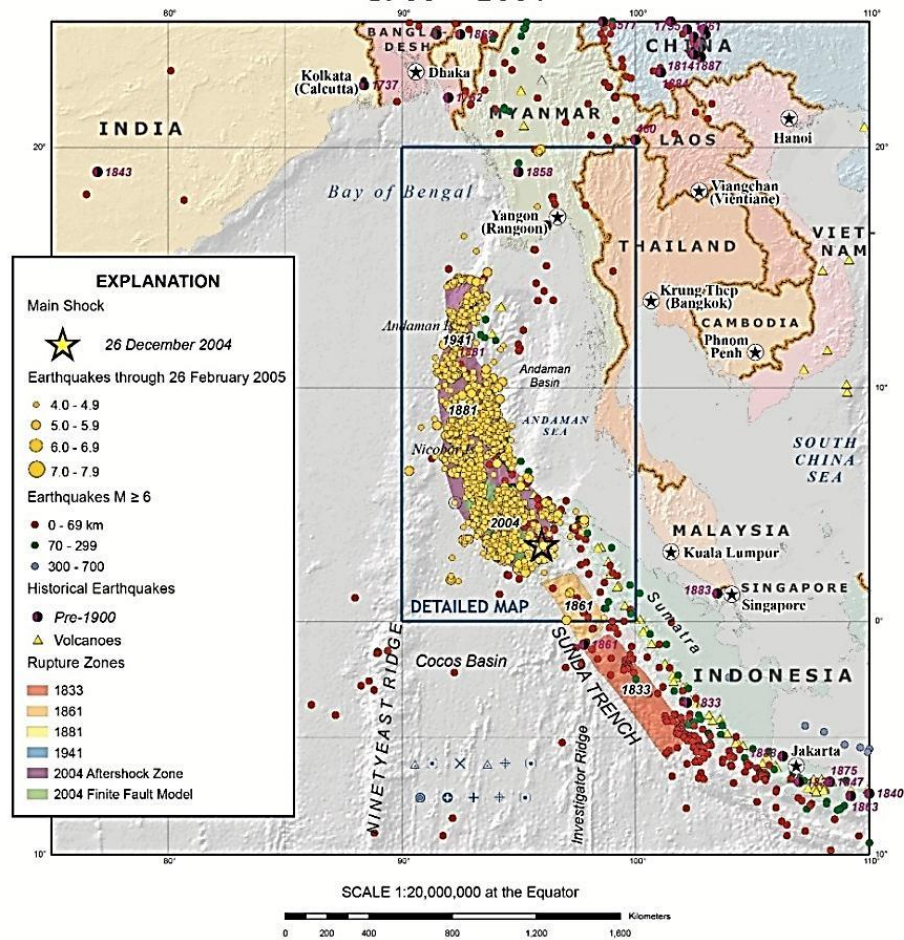


Figure 1.2 The location of the earthquake epicentre in the Sumatera region.

(Page URL: <http://earthquake.usgs.gov/earthquakes/eqarchives/poster/2004/20041226.php> ,

downloaded at 4th Dec 2016)

1.2 Ionospheric Physics

The ionosphere in the Earth-atmosphere system is the E-layer where ionized particles are dense in a region between 90 km to 120 km. From a modelling point of view, this layer can be considered as an atmospheric electro-magnetic system consisting of ions, protons, and electrons. It comprises of low plasma density, in which electrodynamic processes involving charged particles interactions are dynamically happening. Studies in the literature show that the equatorial and low-latitude ionosphere has high

plasma density which is sensitive to electric field perturbation. For example, Fang, Xi, Wu, Liu, and Pu (2016) proposed that electric field and neutral wind can be the essential factors that contribute to the equatorial and low-latitude ionospheric dynamics.

Previous studies investigating the sources of ionospheric disturbances due to seismic activity conclude that two main mechanisms cause the disturbance: 1) electromechanical and 2) acoustic wave. Data from both ground-borne and space-borne observations can be used to investigate the electrodynamics activities in the ionosphere before, during and after strong seismic activities. A recent work discovered that acoustic gravity waves that were generated by strong seismic activity propagate actively in the dynamo region (Oyama et al., 2016). On the other hand, ionospheric disturbances can be caused by solar flares, lightning, and geomagnetic storm. To ensure that the source of disturbance is caused by seismic activity merely, the data collection should be conducted during low solar activity and low geomagnetic storm activity (Ondoh, 2009).

1.3 The Electromagnetic Signal

The electromagnetic (EM) waves that propagate from the surface of the Earth vertically to the ionosphere are known as Earth-ionosphere waveguide. The composition of ionosphere plays a major role when modelling the propagation of electromagnetic waves as earthquake precursor. The numerical pattern of electromagnetic signal propagating through the ionosphere by Extreme Low Frequency (ELF, 3 Hz to 30 Hz), Ultra Low Frequency (ULF, 300 Hz to 3000 Hz) and Very Low Frequency (VLF, 3 kHz to 30 kHz) radio waves can serve as a probe for abstracting the relationship between ionosphere and seismic activity. Radioactive

gases, for example, radon, emanating from strong earthquake preparation zone and ionization in the air become significant, hence increasing electron number density and electric conductivity to generate anomaly to the ionosphere. The dynamical behaviour of an electromagnetic wave propagating in the ionosphere is completely governed by Maxwell's equations. To completely solve Maxwell's equations for this system can be a daunting numerical task. The details of numerical modelling vary greatly depending on the specifics of a numerical scheme and the kind of model adopted.

Electromagnetic phenomena observed prior to and during seismic activity due to the strengthening of the electric field in the ionosphere and have been reported by Sorokin, Yashchenko, and Hayakawa (2007). The modelling of electromagnetic wave propagation to investigate the possibility of earthquake precursor associated with ionospheric disturbance may verify the disturbance observed by the ground station and satellite sensor that occurred before the large earthquake.

There have been several missions launched into orbit using VLF to monitor earthquake as well as the ground-based station (Ho, Jhuang, Su, & Liu, 2013; Ono et al., 2012). These are useful apparatus that can be exploited to investigate, observe and monitor earthquake activity for the precursor. Satellite data on South East Asia region can be used as raw data to model earthquake precursor computationally.

1.4 FDTD Modelling

There are many approaches and techniques to model and simulate vertical electric field in the ionosphere, e.g., waveguide mode theory, frequency-domain mode theory and Finite Different Time Domain (FDTD) method. FDTD is a reliable and robust method that can be applied in a wide area of physical systems, covering

from nano-technology to planetary environment modelling. FDTD method is capable of solving large, complicated physical problems, provided sufficient computational sources, both regarding time and hardware, and is available. The computational resources issues become less pressing with the availability of powerful computers, large data storage and a large amount of Random Access Memory (RAM). The theoretical fundamental of the FDTD method is solidly established and can be easily understood. All these considerations make FDTD a very popular tool for simulating electro dynamical systems.

Common techniques used in ground-based and space-borne observations only provide short-term and discontinuous monitoring of the lower ionosphere and often impractical to implement in many regions of the world. To date, there is no model of simulation of the vertical electric field to study electromagnetic waves propagation via FDTD over Sumatera-Malaysia region. In this thesis, FDTD has been chosen as a technique to model propagation of vertical electric field in the ionosphere with the anomaly in electron density profile that is believed to occur before some large earthquake.

In this study, Sumatra-Andaman Island earthquake that occurred on 26th December 2004 is chosen for our case study simulation of electromagnetic wave propagation in the ionosphere above Aceh, Sumatera and Peninsular Malaysia. The idea is to simulate electromagnetic wave propagation from a VLF source on the ground through the ionosphere up to a vertical height of 120 km. The EM wave moving through its propagation course will undergo interactions with the atmospheric medium, and be detected at various sites on the ground separated at distances within 600 km. Figure 1.3 shows the relationship between pre-earthquake activity on the ground and appearance of disturbance in the lower part of the

ionosphere and the electromagnetic wave propagation. A most definite aspect of this disturbance is caused by deviations in ionospheric parameters.

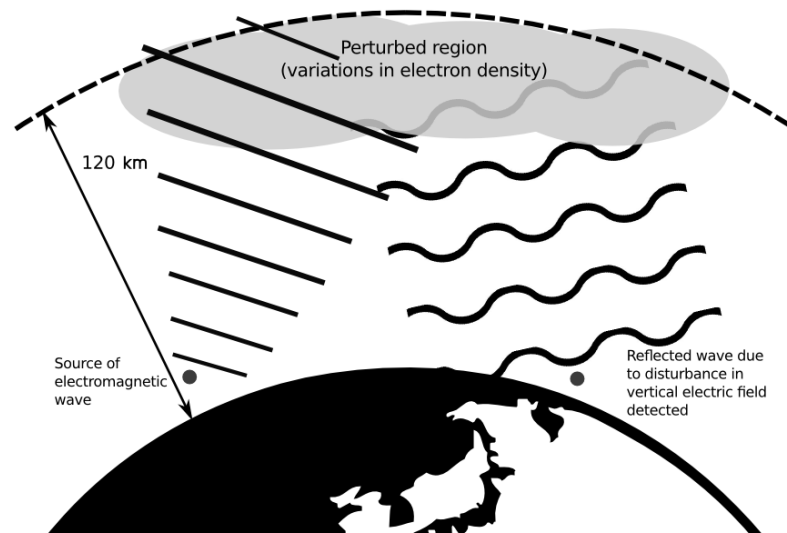


Fig 1.3 The electromagnetic wave propagation from a ground source through the atmosphere up to a height of 120 km where the ionosphere resides.

1.5 Research Questions

This thesis aims to model electromagnetic wave propagation in the ionosphere to study the vertical electric field behaviour under seismically perturbed conditions. Researches on the earthquake, though a common endeavour in many parts of the world, is not common in Malaysia owing to the fact that earthquake rarely occurs in this part of the world. In addition, relevant data is limited. Development of models to study electromagnetic wave propagation in ionosphere for earthquake precursor over the Malaysia-Sumatera region in particular not only has practical relevance but itself a novel research topic in the Malaysian context.

The research is conducted to answer the following questions:

1. Can the perturbation in the electromagnetic signals in the Earth-ionosphere waveguide caused by a large earthquake be effectively simulated via computational means coupled with measured data?
2. Can the computational simulation serve as an effective earthquake precursor?

This thesis revolves the main theme of developing a two dimensional finite difference time domain (2D FDTD) computational model by solving the full Maxwell's equations for VLF band. In this study, simulation for the vertical electric field, before and during an earthquake will be performed. The main aim is to use the model to analyse the variations in the vertical electric field propagating in the background medium (atmosphere) which electron density varies as a function of height. By feeding in empirical data on the height-varying electron density profile of the atmosphere, this approach allows us to investigate the ionosphere anomalies, in an *in-silico* manner, over the Malaysia-Sumatera region near to Aceh 2004's earthquake epicentre. The electron density profile is extracted from database of Challenging Minisatellite Payload (CHAMP) satellite.

1.6 Problem Statements

Human activity on the ground and conductive ionosphere of the Earth and gamma-ray from outer space influence the signal propagation from the ground. The observations of the vertical electric field, E_z at the Earth's surface within an earthquake epicentre zone under quiet and perturbed conditions have been conducted significantly (Bhattacharya, Sarkar, Gwal, & Parrot, 2009; Błęcki, Parrot, & Wronowski, 2010; Itoh, Ando, & Hayakawa, 2013; Naidu, Latha, Rao, & Devi, 2017). The physical mechanism of such perturbations on the vertical electric field, E_z prior to the earthquakes is a poorly investigated problem. Seismic waves can be

detected in the Earth's atmosphere and ionosphere; however, the mechanism of how seismic waves modified the ionosphere in the dynamo region is still an unresolved issue that has no general consensus. Obtaining an earthquake precursor has an obvious practical appeal but is pragmatically yet an unachieved goal. In particular, to obtain an earthquake precursor based on electromagnetic information in the ionosphere is a viable approach many have tried but more research into this area is still required. Numerical and computational study using 2D FDTD model of ionospheric anomalies to simulate vertical electric field around earthquake epicentres have been performed in many parts of the world. However, for Malaysia-Sumatera region, there is hardly any. Malaysia-Sumatera is a seismically active region known as 'Pacific Ring of Fire'. Modelling earth-quark-induced electromagnetic anomaly in the atmosphere of this region is hence warranted.

In addition, depending on the environment (a.k.a. medium) of a particular system to investigate, the complexity of the FDTD code varies tremendously. For example, it is relatively simple to develop a 2D FDTD numerical code for linear, isotropic, non-dispersive medium in a rectangular coordinate system with space-varying medium characteristics. However, for an anisotropic, dispersive medium such as ionosphere, the numerical algorithm to achieve a robust output based on the spirit of FDTD can be non-trivial due to the inherent numerical complexity of Maxwell's equations in such a medium. The variation in the physical properties of the ionospheric as a function of altitude is also a source that compounds the numerical complexity of the problem.

1.7 Research Objectives

This research is aimed to achieve the following objectives:

- 1) To identify the variation in the atmospheric electron density profile near the epicentre region in South East Asia during the 2004 Sumatra earthquake using CHAMP satellite data.
- 2) To develop a home-grown 2D FDTD algorithm and an absorbing boundary condition for the propagation of EM wave in the anisotropic and inhomogeneous ionosphere.
- 3) To apply the 2D FDTD algorithm of electromagnetic wave propagation in the ionosphere that extends to an altitude of 120 km from the Earth's surface and a total horizontal distance of 600 km to construct a protocol for earthquake precursor.

1.8 Scope of Study

The 2D FDTD simulations performed in this thesis are limited to model only the ionosphere conditions during the quiet and perturbed time for the South East Asia region during the 2004 Sumatra earthquake. Data on the electron density profile of the atmosphere taken by a satellite operated during the earthquake time span will be applied. The simulation grid will cover from the ground up to the lower E-layer of the ionosphere (90 – 120 km). In the FDTD simulations, the wave source is an EM spherical wave of low-frequency, $f = 30$ kHz and wavelength $\lambda = 10\ 000$ m. The simulation region has a fixed space grid of size $\Delta x = 1000$ m, covering a total horizontal distance of 600 km and altitude of 120 km. The electron density, N_e data, as a variable parameter in FDTD codes, is the data from the CHAMP satellite. Perfectly Matched Layer (PML) is used to set up an absorbing boundary condition (ABC) at the boundaries of the computational grid.

The curvature of the Earth is assumed to have no influenced the sky wave propagation and hence neglected. This is a reasonable approximation as the radius of the Earth, $R_E = 6400$ km, is an order of magnitude larger than the largest length scale in the simulation. The computational grid is set as a flat, vertical, 2D plane. Rectangular (Cartesian) coordinate system is adopted. The area studied in this thesis is not easily investigated using ground-based data due to poor resolution and large error inflicting ground sensors. Rocket or sounding rocket experimental set-up provides data with a better accuracy but limited in temporal and geographical distribution. Hence the simulations done in this thesis shall not make use of the data taken from these sources.

1.9 Significance of the Study

Very strong earthquakes of magnitude above 7 Richter scale can destroy cities or densely populated areas. The damage could be very significant. The devastation of the building, loss of life and fires may lead to the loss as major as a nuclear explosion. In 26th December 2004, a large earthquake occurred near Aceh, Sumatera in epicentre $3.36^\circ\text{N } 95.85^\circ\text{E}$ at 00:58 UTC followed by a large tsunami and caused complete destruction of Aceh. It was reported that almost 230 000 are dead and more than 500 000 people are missing. The country nearby such as Malaysia, Thailand, Sri Lanka, India, Maldives and Somalia also affected by this earthquake. The study of the earthquake in Southeast Asia region as important as any study conduct all over the world because the earthquake and tsunami will give effect to Indonesia, Malaysia, Thailand, India and leave impacts to socio-economic to the country respectively.

In Malaysia, a study about the earthquake is still at infancy level because the earthquake is not a significant disaster as compared to flood. However, what happened in Kuala Muda, Kedah and Batu Ferringhi, Pulau Pinang during Aceh Earthquake on 2004 as well as the current event of the earthquake in Ranau, Sabah on 2015 should be a motivation to enhance research activities on the earthquake in Malaysia. It is very important and remarkable to study the earthquake activity in Sumatera-Malaysia region for the future to help and develop the human capacity to handle earthquake impact and to mitigate future earthquake as well as the tsunami. This study will give significant impact to the socio-economic well-being of the region. Recently there have been some researches on earthquake study in the Malaysia-Sumatera region. These are mostly research activities centred on data obtained from GPS-TEC and radiosonde station (Bagiya et al., 2017; Devi et al., 2018; A. M. Hasbi, Mohd Ali, & Misran, 2011; Alina Marie Hasbi et al., 2009; Shinagawa, Iyemori, Saito, & Maruyama, 2007; Tao et al., 2017) However, numerical and computational approaches of the ionospheric anomalies phenomena prior to earthquake over the south-east Asia region has been scarce if not totally absent.

The modelling of an electromagnetic anomaly in ionosphere before large earthquake using pure numerical technique can be a useful tool to predict the behaviour of earth magnetic and vertical electric field a few days or hours before the earthquake occurs. A computational approach to model localized region around the epicentre of the earthquake is relatively easy and cheap to implement. The results from this study can possibly lead to an improvement and advancement of research for earthquake precursor and disaster monitoring over the South-east Asia region, specifically.

1.10 Originality Contribution

This thesis presents novel contribution in the following areas:

1. FDTD simulation for electromagnetic propagation in ionosphere during the 2004 Sumatra earthquake using the electron density data recorded from the Challenging Minisatellite Payload (CHAMP) satellite during the seismic event.
2. Code development and implementation of current density, J and electric field, E (J-E) convolution technique to realise FDTD simulations and implementation of a working Perfectly Matched Layer (PML) algorithm in the FDTD code that is specifically tailored for the anisotropic condition found in the ionosphere with inhomogeneous parameters
3. Development of a protocol to construct an earthquake precursor based on FDTD simulations coupled with satellite data on atmospheric electron density profile.

1.11 Organization of Chapter

Chapter 1 of this thesis provides a concise introduction to this research. In addition, this chapter addresses the background, problem statements, research objectives and the significance of the study. Chapter 2 provide a literature review on the research-related works, such as seismo-ionospheric coupling, vertical electric field study and FDTD modelling of the ionosphere. Chapter 3 describes the methodology and the principles of the FDTD technique in detail. The techniques used to simulate the wave propagation through the ionospheric medium via FDTD are also elaborated. Data collection, measurement and processing for further analysis

will also be detailed in this chapter. Chapter 4 consists of a discussion on the analysis of the electron density data in the South-East Asia region before, during and after the earthquake event. The data analysis from the satellite is presented, and results are discussed. Chapter 5 discusses resolve around the implementation of absorbing boundary condition (ABC) in the 2D FDTD code to propagate electromagnetic wave in the anisotropic ionosphere. The performance of the ABC implemented in the FTDT code is then analysed and accessed. Chapter 6 presents the results generated by the home-grown 2D FDTD code that models the EM propagation in the local Earth-ionosphere using satellite data obtained during the 2004 Sumatra earthquake period. The results of the simulations are then examined and analysed. Finally, the conclusion and suggestions for future work are presented in Chapter 7.

CHAPTER 2

LITERATURE REVIEW

2.1 Ionosphere and Ionospheric Disturbance

The ionosphere is a region where the highly ionized particle is developed as a result of the solar radiation ionized the particle within this region. This region has 3 main layers, which are D layer (50 – 90 km), E-layer (90 – 120 km) and F layer (120 – 300 km). The E-layers are divided according to the chemical composition, temperature and level of ionization of the region. The ionospheric disturbance is defined as any anomaly in the ionization level occurred in the ionosphere either in day or night, and detected using high frequency (HF) Doppler sounding, ground-based sensor and satellites.

Previous research have found that ionized particle, ion and electron profile in the ionosphere can be easily disturbed due to solar activities (Buresova, McKinnell, Lastovicka, & Boska, 2011; Guyer & Can, 2013; Sergeenko, Rogova, & Sazanov, 2009) and geomagnetic storm (Hamzah S.Z., 2018; Kumar & Parkinson, 2017; Laštovička, 1996; Polekh et al., 2017; Rees, 1995). However, a few other findings also suggest that despite low solar activity and minor geomagnetic storms, ionospheric disturbance can still be detected by ground-based sensors and satellites (Kherani, Lognonné, Kamath, Crespon, & Garcia, 2009; Kon, Nishihashi, & Hattori, 2011; J. Liu et al., 2010; Oyama et al., 2016; S. A. Pulinets & Legen'ka, 2003; Zakharenkova, Krankowski, & Shagimuratov, 2006)

In addition, in the equatorial and low latitude regions, the existence of Equatorial Ionization Anomaly (EIA), which is highly influenced by solar activity

effects, can provide a more refined observation on the electron density in the ionosphere, from which disturbance due to seismic activity can be accessed (Pundhir, Singh, Singh, & Gupta, 2017). Atmospheric tides in E-layer moves ion, but electron remains in ionosphere because of their high gyro-frequency/collision frequency ratio. Thus makes electron fixed to magnetic and induced current. A polarization electric field is formed immediately to preserve the non-divergent flow of total electric current in agreement with Maxwell's equation. This event is known as E-layer dynamo region and then generates an electrically conductive E-layer (J. M. Forbes et al., 2008). Electrically conductive masses of air interact with Earth's magnetic field, producing intense current in the E-layer of the ionosphere (at the altitude of 85-120 km). This is known as equatorial electrojet (EEJ) (Jeffrey M. Forbes, 1981). The electric field in this region is generated day and night, moves perpendicular to the magnetic field, and produce $\vec{E} \times \vec{B}$ drift. A particle of charge q , mass m , and with velocity \vec{v} , moving in the presence of an external magnetic field, \vec{B} and electric field, \vec{E} , experiences an electromotive force, via

$$m \frac{d\vec{v}}{dt} = q\vec{E} + q(\vec{v} \times \vec{B}). \quad (2.1)$$

In steady state motion, the time derivative of the velocity is small, and in Earth's magnetic field, the electric field \vec{E} is perpendicular to both \vec{v} and \vec{B} . Thus Eq. (2.1) is reduced to

$$\vec{v} = \frac{\vec{E} \times \vec{B}}{|\vec{B}|^2}. \quad (2.2)$$

By referring to (2.2), when the magnetic field is horizontal, the plasma moves in vertical and eastward ionospheric produced, this formation known as equatorial fountain effect (Wu, Liou, Shan, & Tseng, 2008). This effect is causing an anomaly on the ionospheric behaviour, known as Equatorial Ionization Anomaly (EIA). In the last few years, there has been a growing interest in the study to investigate the correlation between EIA in low-latitude ionosphere and seismo-ionospheric coupling for earthquake monitoring (Depueva, 2012; Devi, Medhi, Sarma, & Barbara, 2013; Devi et al., 2018; Klimenko, Klimenko, Zakharenkova, & Pulinets, 2012; Pundhir et al., 2017).

2.2 The Ionospheric Parameter

The main parameters that characterize the ionosphere are electron density, N_e (electron/m³) and the electron collision frequency, ν (s⁻¹) (Nicolet, 1953). N_e is the electron concentration at a point in space, and is normally in the function of height, h , and electron collision frequency ν , which is the rate of collision between single charged particle and neutrally charged atmospheric molecules. The latter defines the conductivity profile in this layer, and is directly related to another parameter, the plasma frequency, ω_p (see Eq. 2.4). The plasma frequency is the natural frequency of plasma oscillation. In addition, the other main parameters are Earth's natural magnetic field B_0 (Tesla, T) and the gyro-frequency, or cyclotron frequency, ω_b . The frequencies are in unit of Hertz, s⁻¹ (Wiesemann, 2014).

The conductivity profile of the ionosphere is a function of electron density and collision frequency. The conductivity parameter, ω_r is defined as

$$\omega_r = \frac{e^2 N_e(h)}{\varepsilon_0 m_e \nu(h)}, \quad (2.3)$$

Plasma frequency, ω_p is defined as

$$\omega_p = \sqrt{\frac{N_e(h)e^2}{m_e \varepsilon_0}}, \quad (2.4)$$

where e is electron charge, m_e is electron mass and ε_0 is permittivity of free space. ν describes the collision rate at which the ions and electrons collide among themselves in a weakly ionized plasma. Electromagnetic waves is related to electron's mass, it will be assumed that the ionosphere to be modelled, the ionic collisions will be neglected, and the collision frequency is contributed mainly by the electronic component (Carlson & Gordon, 1966; Titheridge, 1972). In this thesis, the theoretical model of the collision frequency in the ionosphere by Budden (1985), which assumes a dependence on the altitude via the following relation, is adopted:

$$\nu(h) = 1.816 \times 10^{11} \exp(-0.15h), \quad (2.5)$$

where h is altitude in km and $\nu(h)$ is in unit of Hertz (s^{-1}). Meanwhile, theoretically, the electron density $N_e(h)$ is assuming the following form,

$$N_e(h) = 1.4276 \times 10^7 \exp[\beta(h - h') - 0.15h] \quad (2.6)$$

with β in unit of km^{-1} and h' in unit of km and $N_e(h)$ is in unit of cm^{-3} . The parameter h' control the altitude and β control the sharpness of the profile. During the nighttime Bickel, Ferguson, and Stanley (1970) discovered $h' = 85$ km and $\beta =$

0.5 km^{-1} gave a good agreement for the observation and Thomson (1993) found that for daytime observation, $h' = 70 \text{ km}$ and $\beta = 0.3 \text{ km}^{-1}$ is consistent for measurement.

The conductivity and plasma frequency are related via

$$\omega_r = \frac{\omega_p^2}{\nu(h)}. \quad (2.7)$$

In the anisotropic medium of the ionosphere, the cyclotron, or gyro-frequency, ω_b , is defined as the angular frequency of the circular motion of an electron. Free electron, ions and charged particles are attracted by the Earth's magnetic field, and they move in spiral lines along the magnetic field lines in certain velocity (Schunk & Nagy, 2009). The gyro-frequency determine by the following equation:

$$\omega_b = \frac{eB_0}{2\pi m_e}. \quad (2.8)$$

The data of Earth's natural magnetic field B_0 can be obtained from International Geomagnetic Reference Field (IGRF) (<http://wdc.kugi.kyoto-u.ac.jp/igrf/point/index.html>) provided by International Association of Geomagnetism and Aeronomy (IAGA). IGRF provides global Earth Magnetic Field model data for all locations on Earth. The natural magnetic field for this thesis is based on that located at 3.31° N , 95.85° E , the epicenter of the Sumatra 2004 earthquake.

By referring to the equation in Eq. (2.4), the plasma frequency ω_p depends only on the variable N_e , whereas the other parameter in the equation (e , m_e and ϵ_0)

are all constants. Thus, N_e will be the essential variable parameter for modeling electromagnetic wave propagation in the ionosphere. The acquirement and processing of electron density data will be explained in the following subsection.

2.3 Seismo-Ionospheric Coupling

The history of seismo-ionospheric coupling started in 1971 when Antselevich (1971) observed critical frequency of E-layer and its variation prior to the Tashkent 1966 earthquake. Large nuclear explosion, large volcanic eruption, earthquake with magnitude of 7.0 or larger, as well as rocket launcher are found to excite atmospheric waves that reach the ionospheric layers, leading to coupling between neutral atmosphere and ionized plasma that result in the variations in the electron density. For large earthquake, seismic movement of Earth plate generates acoustic and gravity oscillations that propagate upwards to the ionosphere, which disturbance can be detected up to 1000 km (S. Pulinets & Boyarchuk, 2004). Since then an extensive research effort has been devoted to the seismo-ionospheric coupling phenomena and related problems (Eftaxias et al., 2003; Golubkov, Golubkov, Ivanov, Bychkov, & Nikitin, 2010; Molchanov et al., 2004; S. Pulinets, 2004; Zhao, Zhang, Zhao, & Shen, 2014). Figure 2.1 suggests the processes involved in the physical mechanism of seismo-ionospheric coupling as proposed by S. Pulinets (2004). Figure 2.1 shows ionosphere disturbance originates from radioactive radon gases emanation released during an earthquake. Kelley (2009), Miklavčić et al. (2008) and (Ryu et al., 2016) found similar observation on anomalous radon concentration in soil and water near the active region of earthquake a few weeks or months before large earthquake. It was observed that the concentration level of radon was high, indicating some fault activities were occurring underground.

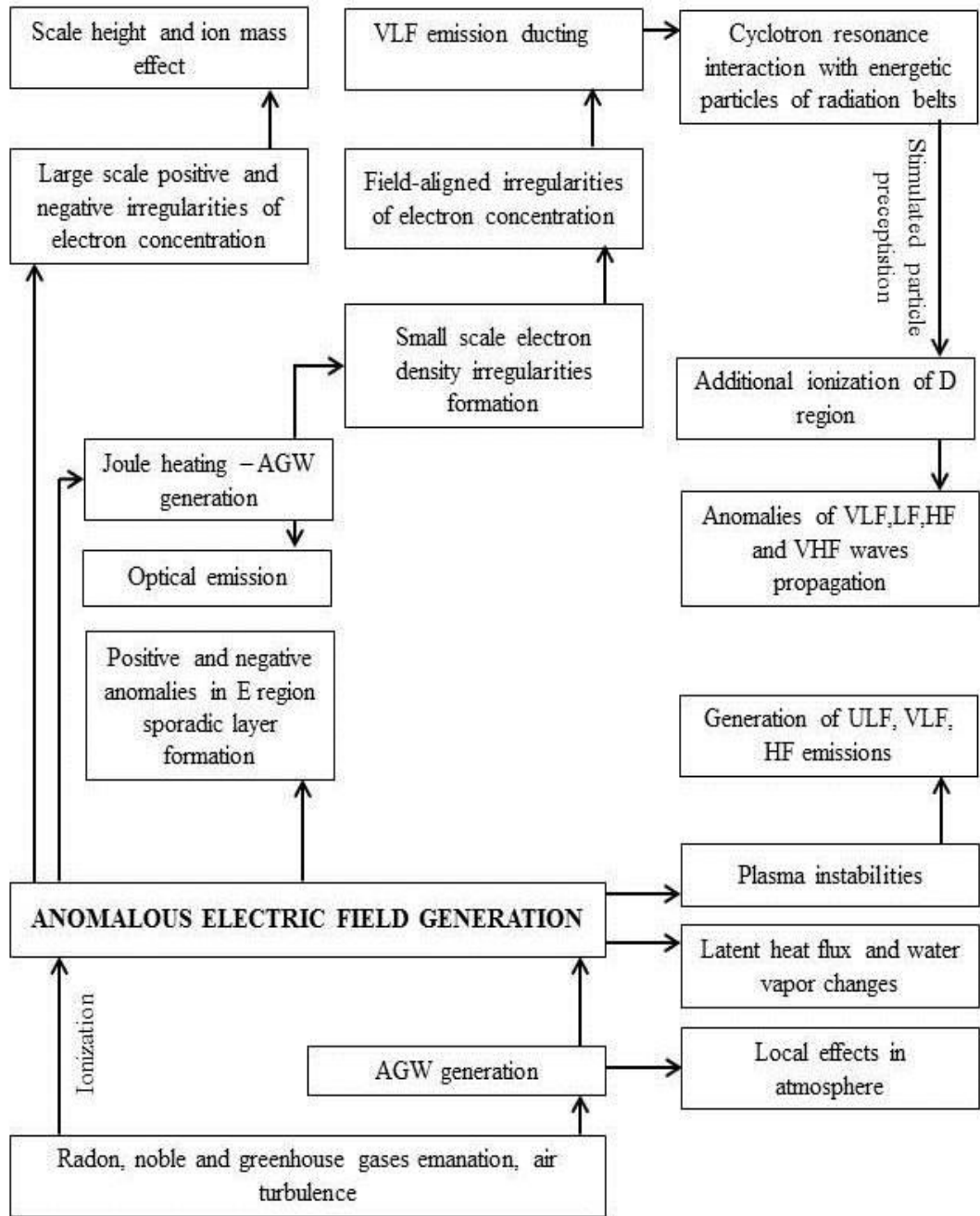


Figure 2.1 Physical mechanism of seismo-ionospheric coupling (S. Pulinet, 2004)

However, the physical mechanism of seismo-ionospheric still has not been completely clarified and needs more detailed study. So far, the most popular idea is acoustic gravity wave (AGW). Several studies have found acoustic gravity wave generated near the earthquake preparation zone prior to and during the large earthquake (Afraimovich, Perevalova, Plotnikov, & Uralov, 2000; Kherani et al., 2012; Sun et al., 2016). The AGW can be observed and detected through a few methods such as Total Electric Content (TEC) measured by Global Positioning System (GPS) receiver (A. M. Hasbi et al., 2011; Tao et al., 2017; Vita, Putra, Subakti, & Muslim, 2017), space-borne Extremely Low Frequency/Ultra Low Frequency/Very Low Frequency (ELF/ULF/VLF) transmitter (Bhattacharya et al., 2009; Błęcki et al., 2010; Ho et al., 2013; Ibanga, Akpan, George, Ekanem, & George, 2017; Sarkar, Choudhary, Sonakia, Vishwakarma, & Gwal, 2012; Zeng, Zhang, Fang, Wang, & Yin, 2009), HF Doppler sounding (Chum et al., 2016; J. Liu et al., 2006), ionosonde (J. Liu, Chen, Pulinets, Tsai, & Chuo, 2000; Maruyama, Tsugawa, Kato, Ishii, & Nishioka, 2012; Maruyama, Yusupov, & Akchurin, 2016) and ground based VLF transmitter (Chakraborty, Sasmal, Chakrabarti, & Bhattacharya, 2018; Hayakawa et al., 2012; Potirakis, Contoyiannis, Asano, & Hayakawa, 2018; Singh, Singh, & Pundhir, 2017).

One of the common ionospheric parameters that are used to characterize the variations in ionosphere due to the AGW is known as Total Electron Content (TEC). It is the electron density measured by GPS receiver that integrates the signal sources from both satellite and ground receiver (Devi et al., 2018; A. M. Hasbi et al., 2011; Heki et al., 2006; Kathuria, Grover, Ray, & Sharma, 2017; Kon et al., 2011). These sources include satellite probes such as Detection of Electro-Magnetic Emissions Transmitted from Earthquake Regions (DEMETER) and CHAMP, as well as HF

Doppler Sounder from ground based (Artru, Farges, & Lognonné, 2004; Gwal, Jain, Panda, & Gujar, 2011; Sun et al., 2016). The findings demonstrate that the variation of ionospheric parameters and ionization level can be detected a few hours to a few days before the large earthquake (with magnitude > 6.0) occurs. As a conclusion, electron density is a prime parameter required for ionosphere modelling.

2.4 The E-layer of Ionosphere

The E-layer in the ionosphere is characterized by means of electron concentration (Appleton, 1927). The E-layer can be described by the Chapman layer (Chapman, 1931) and located at heights between 90 to 120 km. In E-layer, the ionization is caused mainly by Extreme Ultra Violet (XUV) from 80 nm to L-beta and X-rays in the 8-10.4 nm range (Schunk & Nagy, 2009). The dominant ionized particles are O_2^+ and NO^+ . Typically the electron concentration of the E-layer vanished after sunset, leaving very low electron concentration at night. Whitehead (1961) named this layer as sporadic E-layer or Es that remains weakly ionized during at night (Zolesi & Cander, 2014). The convergence of the vertical flux of metallic ions that are believed origin from the meteor, such as Fe^+ and Mg^+ caused the formation of Es layer (S. Pulinets, 2004).

The E-layer also very sensitive to the atmospheric gravity waves (Kaladze, Tsamalashvili, & Kaladze, 2011). Since the 1960s, the scientists discover vertically propagating ionospheric disturbances before the great Alaskan earthquake, detected by HF Doppler (Davies & Baker, 1965; Leonard & Barnes, 1965; Row, 1966). The acoustic gravity waves appear in the long time period, about 15 minutes and can

travel up to 500 km (Koshevaya, Makarets, Grimalsky, Kotsarenko, & Enríquez, 2005).

The ionospheric E-layer study related to the earthquake must take into account all possible solar and geomagnetic to ensure any anomaly can be measured for hours to days before the earthquake, precisely. In this study, the solar flux index, F10.7, Kp, Ap and Dst indices are analysed. The F10.7 index is an indicator of solar activity by measuring the noise level generated by the Sun at a wavelength of 10.7 cm at the Earth's orbit (Schmidtke, 1976). The Ap index is a daily coverage for geomagnetic activity and Kp index is 3 hour average for geomagnetic activity. Both index measured by magnetometer at the ground and depend on E-layer Pedersen and Hall conductivities in local ionosphere (Clilverd, Clark, Clarke, & Rishbeth, 1998). The Dst index is a direct measure of the strength of the intensity of the globally symmetrical electrojet in the equatorial plane (Jakowski, Borries, & Wilken, 2012). Dst index is derived from the hourly scaling of low latitude horizontal magnetic variation. Unit for Dst, Kp, and Ap indices are unit of nanoTesla (nT).

In F-layer, both day and night ratio of ion concentration is smaller than E-layer. For the purpose to limit the scope of this research, we selected the electron density profile in E-layer only.

2.5 The CHAMP Satellite

CHAMP is the acronym for the Germany satellite known as CHALLENGING Minisatellite Payload which was launched from Cosmodrome Pbsetsk on July 15, 2000. This satellite occupies the low earth orbit (LEO) in a circular and near polar orbit. The satellite in polar orbit pass over the North and South and cross over South

East Asia 4 times per day, making it suitable to study ionospheric ionization on a global scale. The CHAMP applied the Global Positioning System (GPS) radio occultation technique to profile ionospheric electron density from satellite orbit's height. The on-board payload of CHAMP measures Earth's gravity and magnetic field data. The information of global magnetic field model, temperature and electron density distribution are then derived from the raw data (Jakowski et al., 2002). The GPS data of CHAMP's and the result of data analysis download from the Information System and Data Centre (ISDC) website (<http://www.gfz-potsdam.de/en/home/>).

2.5.1 The CHAMP Radio Occultation Technique

The Earth surfaces that move suddenly in vertical can excite seismo-traveling ionosphere disturbance to cause anomaly in the vertical profile of the electron density, N_e . This vertical movement is detected up to tens to several thousand kilometres height (Nguyen, Furse, & Simpson, 2015; Sun et al., 2016) and monitored from the ionosonde and satellite. The electron density (N_e) data is obtained based on the Radio Occultation (RO) technique. This technique has been applied by the Global Positioning System / Meteorology (GPS/MET) constellation satellite which main mission is to profile the Earth's atmosphere. RO technique is developed for the mission to study atmosphere in Mars in 1960. The potential to use RO technique for atmosphere profiling show in GPS/MET mission that consists of CHAMP, SAC-C (Satellite de Aplicaciones Cientificas-C), GRACE (Gravity Recovery and Climate Experiment), Metop-A and TerraSAR-X (Anthes, 2011).

In the RO technique, signal passes through the vertical gradient of the refractivity in the atmosphere based on time path delays. This occurs when GPS